

## Relativistic calculations for NN- $\Delta$ scattering with pion and $\rho$ exchange

E. E. van Faassen and J. A. Tjon

*Institute for Theoretical Physics, Princetonplein 5, 3508 TA Utrecht, The Netherlands*

(Received 23 March 1983)

The NN scattering Bethe-Salpeter equation is solved for  $T=1$  partial wave amplitudes up to 1 GeV lab energy. Coupling to  $\Delta$  intermediate states is included by  $\pi$  and  $\rho$  exchange, while  $NN \leftrightarrow NN$  interactions are due to combined  $\pi$ ,  $\rho$ ,  $\eta$ ,  $\epsilon$ ,  $\delta$ , and  $\omega$  mesons. Inclusion of  $\rho$  exchange improves agreement with phase shift analysis in a systematic way.

[NUCLEAR REACTIONS Bethe-Salpeter equation, coupled NN- $\Delta$  scattering,  
 $\rho$  exchange, NN  $T=1$  phase shifts.]

### I. INTRODUCTION

Polarized beam pp scattering data<sup>1</sup> show rich energy and spin dependence at intermediate energies, accompanied by a sharp rise in the pion production cross section. Subsequent phase shift analyses<sup>2,3</sup> show counterclockwise looping in the Argand diagrams of the  $^1D_2$  and  $^3F_3$  phase parameters and suggest an interpretation in terms of exotic dibaryon resonances. However, evidence has been presented that the resonance structures found in these channels can as well be reproduced by more conventional mechanisms like the coupling to the inelastic  $NN\pi$  channel. This has been studied in detail by various groups<sup>4-7</sup> within the framework of relativistic three-body models.

In view of the successful description of nucleon-nucleon scattering at energies up to the one pion production threshold by the one-boson-exchange (OBE) model,<sup>8-11</sup> it is natural to investigate whether such a two-particle model can provide a good description of the dynamics at higher energies as well. Since pion production in the intermediate energy region up to  $T_{\text{lab}}=1$  GeV proceeds predominantly through the production of the  $\Delta$  isobar, it is reasonable to extend the OBE model by including the coupling to  $\Delta$  degrees of freedom.

In a series of papers we want to investigate such an isobar model choosing the relativistic Bethe-Salpeter equation (BSE) as the dynamical equation. One of the principal reasons for this choice is the fact that the BSE can readily be extended to satisfy three particle unitarity.<sup>12</sup> In so doing we hope to learn up to what extend three-particle effects are essential for NN scattering. In particular this may be the case for a correct description of pion production processes. Moreover, in this way we avoid the conceptual difficulties encountered in the Faddeev type of equations, such as satisfying the Pauli exclusion principle for intermediate nucleons and including correctly the retardation effects of the one meson exchange diagrams.

In this paper we consider the  $T=1$  channels of NN scattering and include only coupling to the  $\Delta$  states. The  $\Delta$  isobar is treated as an unstable particle with an energy dependent width. In this way the location of the pion production threshold is properly accounted for. As driving force for  $NN \rightarrow NN$  is taken the sum of one boson exchanges as given in Ref. 13 (to be referred to as I). If we assume that the transition interaction  $NN \rightarrow \Delta$  is

described by one pion exchange, the resonance structures in  $^1D_2$  and  $^3F_3$  are well reproduced for reasonable values of the  $N\pi\Delta$  coupling constant, but some state dependent components in the force are missing.<sup>14</sup> Our main objective here is to study the effects of including the rho meson exchange in the transition interaction. Furthermore, our calculation may serve as guidance on the values of the inelasticity parameters, which are not well determined for some partial waves.

The organization of the paper is as follows. Section II describes the choice of the  $\Delta$  propagator in terms of the Rarita-Schwinger spinors. Section III deals with the partial wave reduction of the coupled Bethe-Salpeter equations neglecting the negative energy spinor state correlations. The form of the couplings used in the calculations is given in Sec. IV together with the algebraic procedures of obtaining the various partial waves. Section V contains some details of the method of solution of the BSE, while in Sec. VI the obtained results are discussed. Some concluding remarks are made in the last section. Three appendices finally give details of the helicity formalism, the isospin algebra, and Jacobi polynomials needed in the actual analysis.

### II. THE $\Delta$ GREEN'S FUNCTION

Our starting point is the BSE for NN scattering within a one-boson-exchange model. This model has been shown<sup>11</sup> to give a reasonable description of the phase parameters in the low energy region  $T_l < 280$  MeV. At higher energies pion production processes have to be taken into account. The dominant production mechanism is expected to involve the  $\Delta$  isobar. A possible way of incorporating the  $\Delta$  degrees of freedom is to include coupling to  $\Delta$  and  $\Delta\Delta$  channels.

In this paper we will present results for isospin  $T=1$  only. The  $\Delta\Delta$  channels are then expected to play a minor role since they open up at higher energies than  $\Delta$  channels (thresholds at 1400 MeV and 640 MeV, respectively). The  $\Delta\Delta$  states are therefore excluded at this stage. Their effects will be discussed in a subsequent paper. This leads to a BSE which is represented diagrammatically in Fig. 1. The original BSE for elastic NN scattering is recovered if all diagrams containing  $\Delta$  lines are omitted.

Following VerWest<sup>15</sup> and Green *et al.*<sup>16</sup> the propagation of the  $\Delta$  particle is described in terms of a one particle

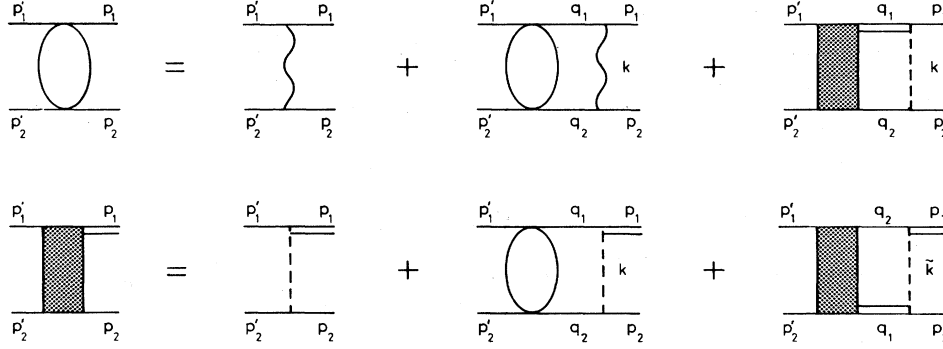


FIG. 1. Diagrammatic representation of the BS equation for coupled channel NN- $\Delta$  scattering. The dashed line indicates  $\pi+\rho$  exchange, and the wiggly line stands for combined  $\pi, \rho, \eta, \epsilon, \delta,$  and  $\omega$  exchange.

model with an energy dependent complex mass. The free propagator of a spin  $\frac{3}{2}$  particle of four-momentum  $(q_0, \vec{q})$  can be written in terms of projection operators as

$$P_{\Delta}^{\mu\nu}(q_0, \vec{q}) = \frac{1}{q_0 - \hat{E}_q + i\eta} \sum_{\sigma} \Delta^{\mu}(\vec{q}, \sigma) \bar{\Delta}^{\nu}(\vec{q}, \sigma) - \frac{1}{-q_0 - \hat{E}_q + i\eta} \sum_{\sigma} W^{\mu}(-\vec{q}, \sigma) \bar{W}^{\nu}(-\vec{q}, \sigma), \quad (1)$$

where  $\sigma = \pm\frac{1}{2}, \pm\frac{3}{2}$ ,  $\hat{E}_q \equiv q^2 + \mu_{\Delta}^2$ , and  $\Delta^{\mu}, W^{\mu}$  are the positive and negative energy Rarita-Schwinger vector spinors, respectively (for explicit expressions see Appendix A). Note that  $\Delta$  and  $W$  depend on the three-momentum only. The effect of negative energy states has been studied in the original NN model and the corrections have been found to be small.<sup>17</sup> In view of this we exclude negative energy states in order to reduce the number of channels involved in the BSE. The pion production process is incorporated by giving the  $\Delta$  mass a negative imaginary part:

$$\mu_{\Delta} = m_0 - \frac{i}{2} \Gamma(q), \quad (2)$$

where  $m_0 = 1236$  MeV. We used the Bransden-Moorhouse parametrization of  $\Gamma$  which reproduces the correct threshold behavior of the  $P_{33}$  resonance:

$$\Gamma(q) = 0, \quad q^2 < 0, \quad (3)$$

$$\Gamma(q) = 2\gamma(\hat{q}R)^3 / [1 + (\hat{q}R)^2], \quad q^2 > 0,$$

with  $\gamma = 71$  MeV,  $R = 0.81$ , and  $\hat{q} = q/m_{\pi}$ . As in Refs. 15 and 16  $q$  is identified with the maximum momentum in the  $\pi N$  subsystem, i.e.,

$$q^2 = [s_{\pi N} - (m_{\pi} - m)^2][s_{\pi N} - (m_{\pi} + m)^2] / 4s_{\pi N}, \quad (4)$$

$$s_{\pi N} = (\sqrt{s} - m)^2,$$

where  $\sqrt{s}$  is the total invariant energy of the NN system. For  $s_{\pi N} = 1236$  MeV Eq. (3) correctly reproduces the experimental  $\Delta$  width  $\Gamma = 120$  MeV. From Eqs. (3) and (4) it is seen that  $\Gamma$  vanishes below pion production thresholds  $s < (2m + m_{\pi})^2$  and that the  $N\Delta$  channels remain closed until pion production starts. It should be noted, however, that, apart from this basic property, the choice of energy

dependence of  $\Gamma$  is not unique: modifications have been proposed taking into account spectator recoil effects.<sup>18</sup>

Moreover, it should be noted that the imaginary part  $\Gamma$  is introduced in the denominator of Eq. (1) only. The  $\Delta$  spinors  $\Delta^{\mu}$  are left unchanged. Although implicitly dependent on  $\hat{E}_q$  and  $\mu_{\Delta}$  the latter are computed with  $\mu_{\Delta} = m_0$  and  $\hat{E}_q = (m_0^2 + q^2)^{1/2}$ .

The single nucleon propagator analogously is truncated to

$$P_N(q_0, q) = \frac{1}{q_0 - E_q + i\eta} \sum_{\sigma = \pm\frac{1}{2}} U(\vec{q}, \sigma) \bar{U}(\vec{q}, \sigma) \quad (5)$$

with  $E_q^2 = m^2 + q^2$ . The nucleon pole always remains on the real  $q_0$  axis, reflecting its stability against decay.

Using these forms of single particle propagators we construct the propagator for two-particle NN or  $N\Delta$  helicity states as defined in Appendix A. We choose the center of mass (c.m.) kinematics to be (see Fig. 1)

$$q_1 = (E + q_0, \vec{q}), \quad p_1 = (E + p_0, \vec{p}),$$

$$p'_1 = (E + p'_0, \vec{p}'), \quad q_2 = (E - q_0, -\vec{q}),$$

$$p_2 = (E - p_0, -\vec{p}), \quad p'_2 = (E - p'_0, -\vec{p}'),$$

$$k = p_1 - q_1, \quad \tilde{k} = p_1 - q_2, \quad E^2 = s/4, \quad (6)$$

and we adopt the convention that the  $\Delta$  is always identified with particle 1. Moreover, a label 1 or 2 will be used to characterize NN and  $N\Delta$  states, respectively.

The  $N\Delta$  propagator  $S_2^{\mu\nu}$  is

$$S_2^{\mu\nu} = P_{\Delta}^{\mu\nu}(1) P_N(2)$$

$$= D_2(q_0, q) \sum_{\lambda_1, \lambda_2} \Delta^{\mu}(q, \lambda_1) \bar{\Delta}^{\nu}(q, \lambda_1) V(q, \lambda_2) \bar{V}(q, \lambda_2)$$

$$= D_2(q_0, q) \sum_{\lambda_1, \lambda_2} |q_0, q, \Omega, \lambda_1, \lambda_2\rangle_2 \langle q_0, q, \Omega, \lambda_1, \lambda_2|_2, \quad (7)$$

$$D_2(q_0, q)^{-1} = (E + q_0 - \hat{E}_q + i\eta)(E - q_0 - E_q + i\eta), \quad (8)$$

where  $\lambda_1 = \pm\frac{1}{2}, \pm\frac{3}{2}$ , and  $\lambda_2 = \pm\frac{1}{2}$ .  $\Delta^{\mu}$  is the particle number 1  $\Delta$  spinor, and  $V$  the particle number 2 nucleon spinor. For definiteness we have explicitly written down the superscript  $\mu, \nu$  for the vector component of  $\Delta$ .

### III. PARTIAL WAVE DECOMPOSITION

The equations corresponding to Fig. 1 constitute a coupled set of linear integral equations. If we assume that the incoming nucleons are on shell, they can be written in the c.m. system as

$$\Phi_{i1}(p_0\vec{p} | 0\vec{p}) = V_{i1}(p_0\vec{p} | 0\vec{p}) - \frac{i}{4\pi^3} \int d^4q \sum_{j=1}^2 V_{ij}(p_0\vec{p} | q_0\vec{q}) S_j(q_0\vec{q}) \Phi_{j1}(q_0\vec{q} | 0\vec{p}) \quad (9)$$

where  $\hat{p} = (E^2 - m^2)^{1/2}$  is the on-shell momentum. Furthermore,  $S_j$  denotes the two particle Green's function for an intermediate state  $j$ , and the four-momenta of the particles were defined in Eq. (6).

The helicity formalism of Jacob and Wick<sup>19</sup> is particularly well suited to make a partial wave decomposition of Eq. (9). We therefore introduce the following states of definite angular momentum  $J$  and spatial parity  $(-)^L$ :

$$|p_0 p J M L S\rangle_i = \left( \frac{2L+1}{2J+1} \right)^{1/2} \sum_{\lambda_1 \lambda_2} \begin{bmatrix} LS & J \\ 0\mu & \mu \end{bmatrix} \begin{bmatrix} S_1 & S_2 \\ \lambda_1 & -\lambda_2 \end{bmatrix} |p_0 p J M \lambda_1 \lambda_2\rangle_i, \quad (10)$$

where  $i=1,2$  again labels the type of state (NN or N $\Delta$ ) and  $S_1, S_2$  are the corresponding spins of particles 1 and 2 in these states. Furthermore,  $\mu = \lambda_1 - \lambda_2$ , and

$$|p_0 p J M \lambda_1 \lambda_2\rangle_i \equiv \left( \frac{2J+1}{4\pi} \right)^{1/2} \int d\Omega D_{M\mu}^{J*}(\Omega) |p_0 p, \Omega, \lambda_1 \lambda_2\rangle_i, \quad (11)$$

where the rotation matrices  $D$  satisfy the orthonormality property

$$\int d\Omega D_{m_1 m_2}^J(\Omega) D_{m_1' m_2'}^{J*}(\Omega) = \frac{4\pi}{2J+1} \delta_{JJ'}. \quad (12)$$

The  $|p_0 p \Omega \lambda_1 \lambda_2\rangle_i$  are the two-particle helicity states defined in Appendix A.

In terms of these we can write the two-particle propagators as

$$S_i(q_0\vec{q}) = D_i(q_0q) \sum_{\lambda_1 \lambda_2} |q_0q \Omega \lambda_1 \lambda_2\rangle_i \langle q_0q \Omega \lambda_1 \lambda_2| \quad (13)$$

with

$$D_1^{-1}(q_0q) = (E + q_0 - E_q + i\eta)(E - q_0 - E_q + i\eta), \quad D_2^{-1}(q_0q) = (E + q_0 - \hat{E}_q + i\eta)(E - q_0 - E_q + i\eta). \quad (14)$$

Using the states (10) and defining

$$\begin{aligned} \tilde{\Phi}_i(p_0 p J L' S') &\equiv \frac{p\hat{p}}{2\pi} {}_i \langle p_0 p J L' S' | \Phi | 0\hat{p} J L S \rangle_1, \\ {}_i \langle p_0 p J L' S' | \tilde{V} | q_0 q J L S \rangle_j &\equiv \frac{pq}{2\pi} {}_i \langle p_0 p L' S' | V | p_0 p J L S \rangle_j \end{aligned} \quad (15)$$

the BSE reduces to

$$\begin{aligned} \tilde{\Phi}_i(p_0 p J L' S') &= {}_i \langle p_0 p J L' S' | \tilde{V} | 0\hat{p} J L S \rangle_1 \\ &\quad - \frac{i}{2\pi^2} \sum_{j=1}^2 \sum_{\tilde{L} \tilde{S}} \int_{-\infty}^{+\infty} dq_0 \int_0^{\infty} dq {}_i \langle p_0 p J L' S' | \tilde{V} | q_0 q J \tilde{L} \tilde{S} \rangle_j D_j(q_0q) \tilde{\Phi}_j(q_0 q J \tilde{L} \tilde{S}). \end{aligned} \quad (16)$$

Here  $\tilde{L} \tilde{S}$  run over all orbital angular momenta and total spins compatible with nonzero Clebsch-Gordan coefficients in Eq. (10). Since the  $\Delta$  isobar carries spin  $\frac{3}{2}$ , N $\Delta$  states have  $S=1,2$ . The  $|JLS\rangle_i$  states for a given value of  $J$  can be classified as in Table I.

The Lagrangians will be chosen invariant under space reflection. Therefore, we have two nonmixing groups of six channels each. Moreover, as discussed in I, one of the uncoupled NN states has odd parity in the relative energy variable and as a result its contribution will vanish in the

nonrelativistic limit. The effect of this state is expected to be small. This is confirmed by actual calculation<sup>17</sup> and we therefore neglect this state along with the negative energy states. This results in a total of five channels for uncoupled NN waves, and six channels for the coupled case.

The solution of the BSE is complicated by the location of propagator singularities near the line of  $q_0$  integration. A Wick rotation over an angle  $\pi/2$  is carried out for all relative energy variables, which changes the integration path to along the imaginary  $q_0$  axis. In the scattering region the rotated equations have additional terms due to the crossing of the imaginary  $q_0$  axis by the nucleon poles in the two particle Green's functions. For the energy region we consider, i.e.,  $T_{\text{lab}} < 1$  GeV, the  $\Delta$  pole in the propagator  $D_2$  (located at  $\omega = \hat{E}_q - E - i\eta$ ) always stays in the fourth quadrant of the  $q_0$  plane. It therefore does not give rise to additional terms. The resulting Wick-rotated equations become

$$\begin{aligned} \tilde{\Phi}_i(ip_0pJL'S') &= {}_i\langle ip_0pJL'S' | \tilde{V} | 0\hat{p}JLS \rangle_1 \\ &+ \frac{1}{2\pi^2} \sum_{j=1}^2 \sum_{\tilde{L}\tilde{S}} \int_{-\infty}^{+\infty} dq_0 \int_0^\infty dq_i \langle ip_0pJL'S' | \tilde{V} | iq_0qJ\tilde{L}\tilde{S} \rangle_j D_j(iq_0q) \tilde{\Phi}_j(iq_0qJ\tilde{L}\tilde{S}) \\ &+ \frac{1}{\pi} \sum_{\tilde{L}\tilde{S}} \int_0^{\hat{p}} dq_i \langle ip_0pJL'S' | \tilde{V} | -\alpha(q)qJ\tilde{L}\tilde{S} \rangle_1 + \langle ip_0pJL'S' | \tilde{V} | \alpha(q)qJ\tilde{L}\tilde{S} \rangle_1 R_1(q) \tilde{\Phi}_1[\alpha(q)qJ\tilde{L}\tilde{S}] \\ &+ \frac{1}{\pi} \sum_{\tilde{L}\tilde{S}} \int_0^{\hat{p}} dq_i \langle ip_0pJL'S' | \tilde{V} | \alpha(q)qJ\tilde{L}\tilde{S} \rangle_2 R_2(q) \tilde{\Phi}_2(\alpha(q)qJ\tilde{L}\tilde{S}), \end{aligned} \quad (17)$$

where

$$\alpha(q) = E - E_q + i\eta$$

is the nucleon number 2 pole position, and

$$R_1(q) = \frac{1}{2(E_q - E - i\eta)}, \quad (18)$$

$$R_2(q) = \frac{1}{E_q + \hat{E}_q - 2E - i\eta}.$$

The single integral contributions in Eq. (17) were expressed in terms of  $\Phi_1$  at  $q_0 = \alpha(q)$  using the symmetry property as discussed in I:

$$\Phi_1(q_0qJLS) = \Phi_1(-q_0qJLS). \quad (19)$$

To solve Eq. (17) we need the auxiliary equation for  $\Phi_j(\alpha(p)pJLS)$  which has precisely the same form as Eq. (17) with the argument  $ip_0$  replaced by  $\alpha(p)$ .

#### IV. COUPLINGS

The  $\Delta$  isobar carries isospin  $\frac{3}{2}$  and it is clear that N $\Delta$  interactions can be mediated by isospin 1 mesons only, the two candidates being the pseudoscalar pion and the vector rho meson. The pion builds up the long range part of the interaction and can account for the resonance structure in  ${}^3F_3$  and  ${}^1D_2$  channels, while the  $\rho$  meson is known to be important for the higher momentum transfers. For the transition Lagrangians we take the customary form,

TABLE I. Quantum numbers for the various channels.

Spatial parity	$S$	$L$	Even $J$	Odd $J$
$(-)^J$				
1 NN	0	$J$	1	0
2 NN	1	$J$	0	1
3 N $\Delta$	1	$J$		1
4 N $\Delta$	2	$J-2$		1
5 N $\Delta$	2	$J$		1
6 N $\Delta$	2	$J+2$		1
$(-)^{J+1}$				
1 NN	1	$J-1$	1	0
2 NN	1	$J+1$	1	0
3 N $\Delta$	1	$J-1$		1
4 N $\Delta$	1	$J+1$		1
5 N $\Delta$	2	$J-1$		1
6 N $\Delta$	2	$J+1$		1

$$\begin{aligned} \mathcal{L}_{N\Delta\pi} &= -\frac{f_{\pi\Delta}}{m_\pi} \bar{\psi} \vec{T} \psi^\mu \cdot \partial_\mu \vec{\Phi} - \frac{f_{\pi\Delta}}{m_\pi} \bar{\psi} \mu \vec{T}^\dagger \psi \cdot \partial_\mu \vec{\Phi}, \\ \mathcal{L}_{N\Delta\rho} &= -i \frac{f_{\rho\Delta}}{m_\rho} \bar{\psi} \gamma^5 \gamma^\mu \vec{T} \psi^\nu \cdot (\partial_\mu \vec{\varphi}_\nu - \partial_\nu \vec{\varphi}_\mu) \\ &\quad - i \frac{f_{\rho\Delta}}{m_\rho} \bar{\psi}^\nu \gamma^\mu \gamma^5 \vec{T}^\dagger \psi \cdot (\partial_\mu \vec{\varphi}_\nu - \partial_\nu \vec{\varphi}_\mu), \end{aligned} \quad (20)$$

where  $\psi$  and  $\Phi$  denote the nucleon and pion fields, respectively.  $\psi^\nu$  is the  $\Delta$  isobar Rarita-Schwinger wave function and  $\varphi_\nu$  stands for the  $\rho$ -meson vector field.  $\Delta\Delta$  vertices are disregarded in view of uncertainties with respect to the coupling Lagrangian. The NN $\pi$  and NN $\rho$  vertices are taken from the previous treatment of the NN interaction:

$$\begin{aligned} \mathcal{L}_{NN\pi} &= ig_\pi \bar{\psi} \gamma^5 \vec{\tau} \psi \cdot \vec{\Phi}, \\ \mathcal{L}_{NN\rho} &= g^V \bar{\psi} \gamma^\mu \vec{\tau} \psi \cdot \varphi_\mu \\ &\quad + \frac{ig^T}{4m} \bar{\psi} \sigma^{\mu\nu} \vec{\tau} \psi \cdot (\partial_\mu \vec{\varphi}_\nu - \partial_\nu \vec{\varphi}_\mu), \end{aligned} \quad (21)$$

where  $\sigma^{\mu\nu} = \frac{1}{2}[\gamma^\mu, \gamma^\nu]$  and  $\tau_i$  are the Pauli matrices operating in isospin space. The effect of the isospin operators  $T$  and  $\tau$  can be reduced to an overall factor for each amplitude. The resulting factors for the various channels

are collected in Appendix B. Isospin operators are omitted from the remaining part of this section.

Using the above Lagrangians and Eq. (6) we get the following:

A. Pion exchange:

$$V_{21} = \frac{f_{\pi\Delta} g_{\pi}}{4\pi \cdot m_{\pi}} \frac{1}{k^2 - m_{\pi}^2} k_{\nu} \bar{\Delta}^{\nu}(\vec{p}_1) U(\vec{q}_1) \cdot \bar{V}(\vec{p}_2) \gamma_5 V(\vec{q}_2), \quad (22)$$

$$V_{12} = \frac{f_{\pi\Delta} g_{\pi}}{4\pi \cdot m_{\pi}} \frac{1}{k^2 - m_{\pi}^2} \bar{U}(\vec{p}_1) \Delta^{\nu}(\vec{q}_1) k_{\nu} \cdot \bar{V}(\vec{p}_2) \gamma_5 V(\vec{q}_2), \quad (23)$$

$$V_{22} = -\frac{f_{\pi\Delta}^2}{4\pi \cdot m_{\pi}^2} \frac{1}{\tilde{k}^2 - m_{\pi}^2} \bar{V}(\vec{p}_2) \Delta^{\mu}(\vec{q}_1) \tilde{k}_{\mu} \cdot \tilde{k}_{\nu} \bar{\Delta}^{\nu}(\vec{p}_1) V(\vec{q}_2). \quad (24)$$

B. Rho exchange:

$$V_{ij} = (V^T + V^V)_{ij}, \quad (25)$$

$$V_{21}^T = \frac{-f_{\rho\Delta} \cdot g^T}{4\pi \cdot m_{\rho}} \frac{1}{2m(k^2 - m_{\rho}^2)} \bar{\Delta}^{\nu}(\vec{p}_1) \gamma^{\mu} \gamma^5 U(\vec{q}_1) \cdot \bar{V}(\vec{p}_2) \sigma^{\rho\tau} V(\vec{q}_2) (g_{\tau\mu} k_{\nu} k_{\rho} - g_{\tau\nu} k_{\mu} k_{\rho}), \quad (26)$$

$$V_{12}^T = \frac{-f_{\rho\Delta} \cdot g^T}{4\pi \cdot m_{\rho}} \frac{1}{2m(k^2 - m_{\rho}^2)} \bar{U}(\vec{p}_1) \gamma^5 \gamma^{\mu} \Delta^{\nu}(\vec{q}_1) \cdot \bar{V}(\vec{p}_2) \sigma^{\rho\tau} V(\vec{q}_2) (g_{\tau\mu} k_{\nu} k_{\rho} - g_{\tau\nu} k_{\mu} k_{\rho}), \quad (27)$$

$$V_{12}^V = \frac{f_{\rho\Delta} \cdot g^V}{4\pi \cdot m_{\rho}} \frac{1}{k^2 - m_{\rho}^2} \bar{\Delta}^{\nu}(\vec{p}_1) \gamma^{\mu} \gamma^5 U(\vec{q}_1) \cdot \bar{V}(\vec{p}_2) \gamma^{\rho} V(\vec{q}_2) (g_{\mu\rho} k_{\nu} - g_{\nu\rho} k_{\mu}), \quad (28)$$

$$V_{21}^V = \frac{f_{\rho\Delta} \cdot g^V}{4\pi \cdot m_{\rho}} \frac{1}{k^2 - m_{\rho}^2} \bar{U}(\vec{p}_1) \gamma^5 \gamma^{\mu} \Delta^{\nu}(\vec{q}_1) \cdot \bar{V}(\vec{p}_2) \gamma^{\rho} V(\vec{q}_1) (g_{\mu\rho} k_{\nu} - g_{\nu\rho} k_{\mu}), \quad (29)$$

$$V_{22} = \frac{f_{\rho\Delta}^2}{4\pi m_{\rho}^2} \frac{1}{\tilde{k} - m_{\rho}^2} \bar{V}(\vec{p}_2) \gamma^5 \gamma^{\mu} \Delta^{\nu}(\vec{q}_1) \cdot \bar{\Delta}^{\rho}(\vec{p}_1) \gamma^{\sigma} \gamma^5 V(\vec{q}_2) (\tilde{k}_{\nu} \tilde{k}_{\sigma} g_{\mu\rho} + \tilde{k}_{\rho} \tilde{k}_{\mu} g_{\nu\sigma} - \tilde{k}_{\mu} \tilde{k}_{\sigma} g_{\nu\rho} - \tilde{k}_{\nu} \tilde{k}_{\rho} g_{\mu\sigma}), \quad (30)$$

where  $k$  and  $\tilde{k}$  are defined in Eq. (6).

The interactions for a given partial wave are computed from these spinor amplitudes. Using Eqs. (10) and (11) we obtain

$${}_i \langle p_0 p J L S' | \tilde{V} | q_0 q J L S \rangle_j = \sum_{\lambda_1 \lambda_2} \frac{[(2L+1)(2L'+1)]^{1/2}}{2J+1} \times \begin{bmatrix} L' & S' & J \\ 0 & \mu' & \mu' \end{bmatrix} \begin{bmatrix} S'_1 & S'_2 & S' \\ \mu'_1 & -\mu'_2 & \mu' \end{bmatrix} \begin{bmatrix} L & S & S \\ 0 & \mu & \mu \end{bmatrix} \begin{bmatrix} S_1 & S_2 & S \\ \mu_1 & -\mu_2 & \mu \end{bmatrix} A_{ij}(\mu'_1 \mu'_2 | \mu_1 \mu_2), \quad (31)$$

$$A_{ij}(\mu'_1 \mu'_2 | \mu_1 \mu_2) \equiv 2\pi \int d \cos \theta {}_i \langle p_0 p(\theta, 0) \mu'_1 \mu'_2 | \tilde{V} | q_0 q(0, 0) \mu_1 \mu_2 \rangle_j d_{\mu\mu'}^J(\theta), \quad (32)$$

where

$$d_{\mu\mu'}^J(\theta) = D_{\mu\mu'}^J(0, \theta, 0).$$

The integrand can always be expressed in terms of Legendre polynomials. (For details see Appendix C.) The angular integration then yields Legendre functions of the second kind, the argument of which depends on the boson propagator:

$$\int \frac{P_l(\cos \theta) d \cos \theta}{k^2 - m_B^2} = \frac{-1}{pq} Q_l(z^-), \quad (33)$$

$$\int \frac{P_l(\cos \theta) d \cos \theta}{\tilde{k}^2 - m_B^2} = \frac{1}{pq} Q_l(-z^+)$$

$$= \frac{(-)^{l+1}}{pq} Q_l(z^+),$$

where

$$z^{\pm} = \frac{p^2 + q^2 + m_B^2 - (p_0 \pm q_0)^2 - i\epsilon}{2pq}. \quad (34)$$

The analytical expressions of the spinor amplitudes  $A_{ij}$  have been computed using the SCHOONSCHIP program<sup>20</sup> for algebraic manipulation. As a check we numerically compared the pion-mediated NN- $\Delta$  amplitudes with those of Ref. 21 for the  ${}^1D_2$  case. This provides a test on the energy shell, but off mass shell. From nonrelativistic scattering theory there exist bounds on the transition amplitudes near threshold,

$${}_i \langle p_0 p J L S' | \tilde{V} | q_0 q J L S \rangle_j = O(p^{L'+2} \cdot q^{L+2}). \quad (35)$$

Furthermore, time reversal invariance implies

$${}_i \langle p_0 p J L S' | \tilde{V} | q_0 q J L S \rangle_j = {}_j \langle q_0 q J L S | \tilde{V} | p_0 p J L S' \rangle_i . \quad (36)$$

Both relations have been tested for all amplitudes.

It should be noted that the expressions (22)–(30) for  $V_{12}$  and  $V_{21}$  lead to diagrams where the  $\Delta$  particle is always coupled to the number 1 nucleon. However, the diagrams should be included where intermediate N and  $\Delta$  particles are interchanged. These exchanged diagrams can readily be included by proper antisymmetrization in the NN channels. Under the particle exchange operator  $P_{12}$  the NN helicity states transform as

$$P_{12} | p_0 p J L S \rangle_1 = (-)^{L+S+T} | -p_0 p J L S \rangle_1 , \quad (37)$$

where  $T$  is the isospin of the state.  $L+S+T$  being odd for the NN states included, the antisymmetrization amounts to

$$\begin{aligned} V_{12}(p_0 p | q_0 q) &\rightarrow \frac{1}{\sqrt{2}} [ V_{12}(p_0 p | q_0 q) \\ &\quad + V_{12}(-p_0 p | q_0 q) ] , \\ V_{21}(p_0 p | q_0 q) &\rightarrow \frac{1}{\sqrt{2}} [ V_{21}(p_0 p | q_0 q) \\ &\quad + V_{21}(p_0 p | -q_0 q) ] . \end{aligned} \quad (38)$$

$$\begin{aligned} I_i(p) &= \frac{1}{\pi} \sum_{j=1}^2 \sum_{\tilde{L}\tilde{S}} \int_0^{\hat{p}} dq \operatorname{Re}(K_{ij}(p, q)) R_j \tilde{\Phi}_j(\alpha(q), q, J\tilde{L}\tilde{S}) \\ &\quad + \frac{i}{\pi} \theta(D) \sum_{j=1}^2 \sum_{\tilde{L}\tilde{S}} \int_{q_-(p)}^{\min(q_+(p), \hat{p})} \operatorname{Im}(K_{ij}(p, q)) R_j \tilde{\Phi}_j(\alpha(q), q, J\tilde{L}\tilde{S}) , \end{aligned} \quad (40)$$

where

$$\begin{aligned} K_{ij}(p, q) &= {}_i \langle \alpha(p) p J L S' | \tilde{V} | -\alpha(q) q J \tilde{L} \tilde{S} \rangle_j \delta_{1j} \\ &\quad + {}_i \langle \alpha(p) p J L S' | \tilde{V} | \alpha(q) q J \tilde{L} \tilde{S} \rangle_j \end{aligned} \quad (41)$$

and  $q_{\pm}$  are the values for  $q$  satisfying Eq. (39) with  $|\lambda| = 1$ . They are given by

$$\begin{aligned} q_-(p) &= \left| \frac{pA - D^{1/2}}{2(p^2 - \chi^2)} \right| , \\ q_+(p) &= \frac{pA + D^{1/2}}{2(\chi^2 - p^2)} , \end{aligned} \quad (42)$$

where

$$\begin{aligned} \chi &= 2E - E_p , \\ A &= \chi^2 + m^2 - m_{\pi}^2 - p^2 , \\ D &= \chi^2 [A^2 + 4m^2(p^2 - \chi^2)] . \end{aligned} \quad (43)$$

The imaginary part of the integral Eq. (40) only contributes for  $D > 0$ , which can be satisfied if  $2E \geq 2m + m_{\pi}$ . For a given iteration,  $\phi$  is known on a fixed set  $S$  of mesh points between 0 and  $\hat{p}$ . To calculate the contribution

As explained in I, fermion statistics is now satisfied automatically.

## V. METHOD OF SOLUTION

The set of coupled integral equations (17) together with the auxiliary equations are solved by first determining the Born series solution and then applying Padé approximants on this series. The calculation of the Born terms proceeds in the same way as in I, except that we now iterate for the  $T$  matrix instead of the  $K$  matrix. As in I the nucleon pole singularities in the NN channels are dealt with by a subtraction. The  $N\Delta$  channels do not need a subtraction since the  $\Delta$  pole does not lie on the path of integrations.

A complication absent at lower energies is the fact that above pion production threshold the driving forces in the single integral of the auxiliary equation may become complex on some part of the integration interval  $[0, \hat{p}]$ . This reflects the possibility of the exchanged pion being produced energetically. It occurs when the argument of the  $Q_l$  functions in the one pion exchange amplitudes lies on the cut  $[-1, 1]$ , i.e., for

$$[\alpha(p) \pm \alpha(q)]^2 = p^2 + q^2 - 2pq\lambda + \mu^2 , \quad \lambda \in [-1, 1] \quad (39)$$

with  $\alpha(p) = E - E_p$ . In view of this the single integral of the auxiliary equation can be written as

from the second term in Eq. (40) Gaussian mesh points are used in the integration interval  $[q_-, \min(q_+, \hat{p})]$  together with cubic interpolation for  $\phi$  given on  $S$ . It should be noted, that although the integrand of the first integral in Eq. (40) contains logarithmic singularities, no special treatment of these was necessary to get stable numerical results.

As in the  $NN \leftrightarrow NN$  interaction, the singular behavior of the  $N\Delta$  amplitudes is regularized by the introduction of dipole form factors. The boson propagators are multiplied by

$$F^2(k^2) = \left[ \frac{\Lambda_{N\Delta}^2}{\Lambda_{N\Delta}^2 - k^2} \right]^2 . \quad (44)$$

The cutoff mass for  $V_{11}$  was kept at  $\Lambda_{NN}^2 = 1.9m^2$  as before, whereas for  $\Lambda_{N\Delta}^2$  a value between  $m^2$  and  $1.5m^2$  was used. From the Born series of Eq. (17) the physical transition element  $\Phi_1(0\hat{p})$  was computed from the (N/N) Padé approximants. As in the case of NN states only the rate of convergence is good. As an example Table II shows results in the case of  $f_{\pi\Delta}^2/4\pi = 0.35$  at  $T_{\text{lab}} = 600$  MeV. The last column gives phase shifts computed from the Born term only. Lacking the attractive contribution of the  $N\Delta$

TABLE II. Rate of convergence of (N/N) Padé approximants for various channels at 600 MeV ( $f_{\pi\Delta}^2/4\pi=0.35$ ,  $f_{\rho\Delta}^2/4\pi=8.0$ ,  $g_{\epsilon}^2/4\pi=5.9$ ,  $\Lambda_{N\Delta}^2=1.5m_N^2$ ). A. Phaseshift  $\delta$ . Last column contains values from Born terms only. B. Inelasticity  $\eta=\cos^2\theta$ .

N	1	2	3	4	5	6	Born
A							
$^1S_0$	-55.0	-41.0	-40.8	-41.0	-41.0	-41.0	-77.8
$^3P_1$	-41.7	-33.7	-32.0	-30.3	-30.4	-30.5	-55.0
$^1D_2$	16.1	13.9	14.1	14.1	14.1	14.1	-1.19
$^3F_3$	-3.76	-3.87	-3.89	-3.89	-3.89	-3.89	-9.48
$^1G_4$	3.96	3.92	3.92	3.92	3.92	3.92	2.03
$^3H_5$	-1.66	-1.66	-1.66	-1.66	-1.66	-1.66	-2.25
$^1I_6$	0.95	0.95	0.95	0.95	0.95	0.95	0.73
B							
$^1S_0$	1.088	1.052	0.999	0.977	0.976	0.976	
$^3P_1$	1.016	0.863	0.835	0.794	0.787	0.787	
$^1D_2$	0.899	0.831	0.814	0.813	0.813	0.813	
$^3F_3$	0.917	0.912	0.911	0.911	0.911	0.911	
$^1G_4$	0.975	0.973	0.973	0.973	0.973	0.973	
$^3H_5$	0.993	0.992	0.992	0.992	0.992	0.992	
$^1I_6$	0.998	0.998	0.998	0.998	0.998	0.998	

box, the latter are consistently too low and do not provide a good approximation for  $J$  as high as 6. Below the one pion production threshold elastic unitarity is well satisfied ( $|\eta-1| < 10^{-4}$  at 200 MeV).

A variety of parametrizations of the NN scattering matrix is in use.<sup>22,23</sup> Here we employ the parametrization of Arndt and VerWest<sup>24</sup>:

$$S_j = \cos^2 \rho_j e^{2i\delta_j} \quad (45)$$

for uncoupled waves, and

$$S = \begin{pmatrix} \cos^2 \rho_1 \cos 2\epsilon' e^{2i\delta_1} & i \cos \rho_1 \cos \rho_2 \sin 2\epsilon' e^{i(\delta_1 + \delta_2)} \\ i \cos \rho_1 \cos \rho_2 \sin 2\epsilon' e^{i(\delta_1 + \delta_2)} & \cos^2 \rho_2 \cos 2\epsilon' e^{2i\delta_2} \end{pmatrix} \quad (46)$$

for coupled triplets. The mixing parameter  $\epsilon' = \epsilon_1 + i\epsilon_2$  is complex, leading to a total of six independent parameters in the coupled case.

## VI. RESULTS

In a previous paper<sup>14</sup> it was shown that coupling to isobar channels using only one pion exchange in the transition interaction could account for the resonant behavior of the  $^1D_2$  and  $^3F_3$  phase shifts. In order to obtain reasonable results it was necessary, however, to resort to a low  $N\Delta$  cutoff value of  $\Lambda_{N\Delta}^2 = m^2$ . Furthermore, the calculated phase parameters of the  $^3P_1$  and  $^3P_2$  waves indicated that a state dependent part of the transition interaction was absent. Since the  $\rho$  exchange is known to have strong state dependence, its inclusion may lead to an improvement.

In Figs. 2–4 are shown some results when  $\rho$  exchange is also included in the transition interaction. The coupling constants for the  $NN \leftrightarrow NN$  interaction are the same as in Ref. 17 except for the  $g_\epsilon^2$  which is adjusted to improve fits to the experimental data. Since the  $\epsilon$  meson affects the intermediate energy range of the nuclear force and the introduction of the coupling to the  $N\Delta$  states leads to an additional attraction in this region, we have in general to de-

crease the value of  $g_\epsilon^2$  to compensate stronger coupling to isobar states. For the results in Figs. 2 and 4 the  $N\Delta$  coupling constants were taken from the quark model predictions,<sup>25</sup> i.e.,

$$\frac{f_{\pi\Delta}^2}{4\pi} = \frac{72}{25} \frac{g_\pi^2}{4\pi} \left[ \frac{m_\pi}{2m} \right]^2, \quad (47)$$

$$\frac{f_{\rho\Delta}^2}{4\pi} = \frac{72}{25} \frac{g^{\nu^2}}{4\pi} \left[ 1 + \frac{g^T}{g^\nu} \right]^2 \left[ \frac{m_\rho}{2m} \right]^2. \quad (48)$$

This leads to the values  $f_{\pi\Delta}^2/4\pi=0.23$  and  $f_{\rho\Delta}^2/4\pi=10.33$ . For reference the results for  $f_{\rho\Delta}=0$  are also shown in the figures.

It is often stated that  $\rho$  mediated  $N\Delta$  coupling gives a short range repulsive contribution weakening the strongly attractive pion interaction. This is seen, for instance, for the channels  $^1D_2$  and  $^3F_3$  where the resonancelike structure is reduced by  $\rho N\Delta$  coupling.

Although this is the general trend, notable exceptions are  $^3P_2$  and  $^3F_4$ . As an important consequence, inclusion of  $\rho$  exchange leads to repulsion in  $^3P_1$  whereas the  $^3P_2$  and  $^3F_4$  channels become more attractive. For all those channels agreement with the experimental phase shifts is improved. This indicates that  $\rho N\Delta$  coupling is an indispensable feature of any realistic isobar model. A similar state dependent effect could not be the result of adjusting parameters in the NN sector, e.g., by altering the  $\epsilon$ -coupling constant.

Most inelasticities are considerably decreased by  $\rho N\Delta$  coupling, a notable exception being again  $^3P_2$ . For this wave the increase in inelasticity is in accordance with the additional attraction we already mentioned.

The second important aspect of  $\rho N\Delta$  coupling is its effect on the regularization: apart from  $P$  waves, there is no significant cutoff dependence left. This is in sharp contrast to the case of  $\pi$  exchange only, where no meaningful fit for  $\Lambda_{N\Delta}^2 = 1.5m^2$  could be found. Figures 3 and 4 show results for  $f_{\pi\Delta}^2/4\pi=0.35$ , which is suggested by pionic decay of the  $P_{33}$  resonance.<sup>27</sup> This value is corroborated by the Chew-Low result<sup>25</sup> of 0.32. The  $\rho N\Delta$  coupling constant is taken to be  $f_{\rho\Delta}^2/4\pi=8.0$ . For fitting to

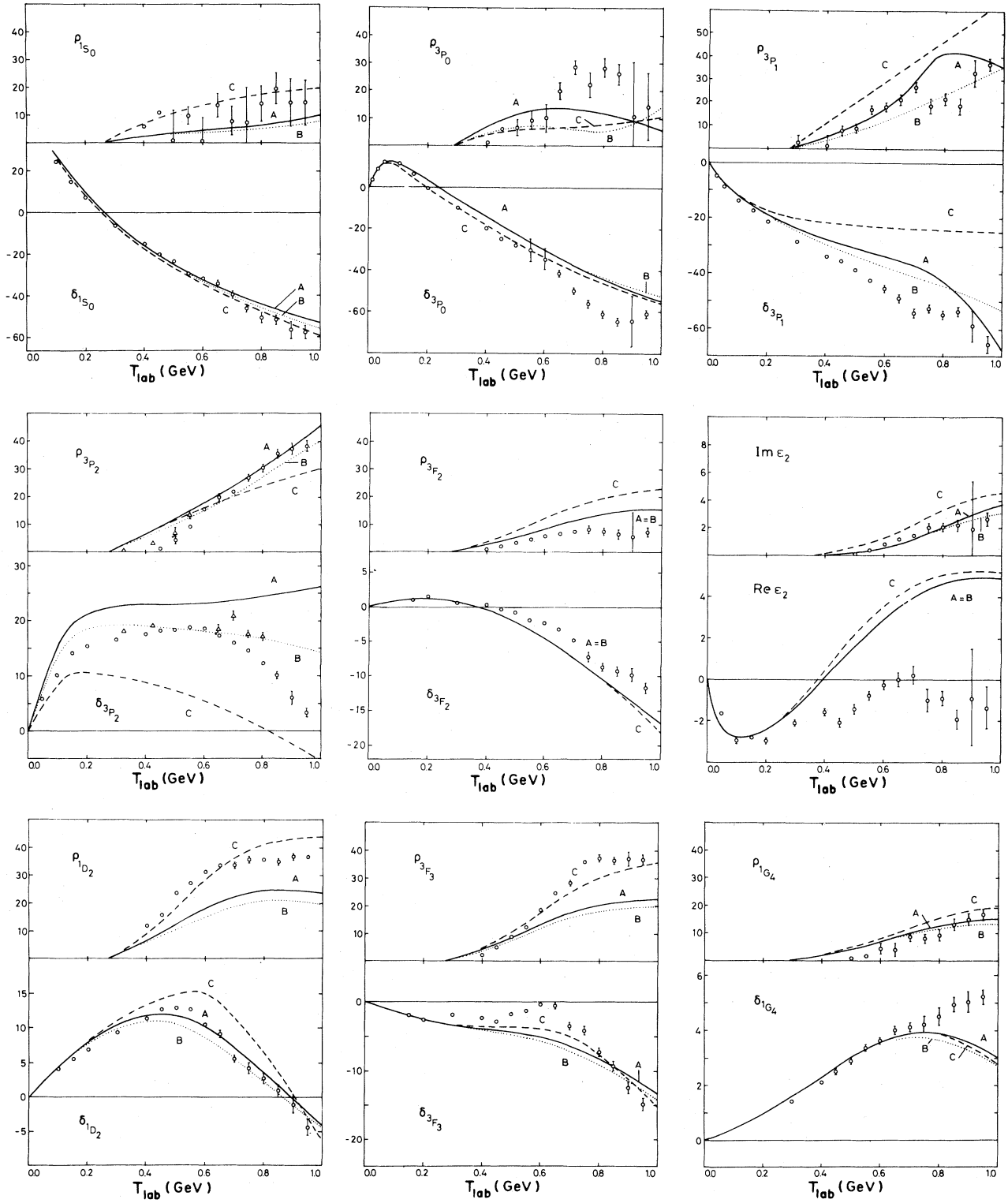


FIG. 2.  $T=1$  NN phase parameters  $\delta$  and  $\rho$  in degrees for quark model  $\Delta$  coupling constants:  $f_{\pi\Delta}^2/4\pi=0.23$ ,  $f_{\rho\Delta}^2/4\pi=10.33$ . ( $g_e^2/4\pi$ ,  $\Lambda_{N\Delta}^2/m^2$ ) is (7.3, 1.5) for curve A and (7.3, 1.0) for curve B. Curve C is obtained with (5.9, 1.0) and  $\rho N\Delta$  coupling set to zero. Experimental phase shift data are taken from Ref. 3 (open circles) and Ref. 24 (triangles).



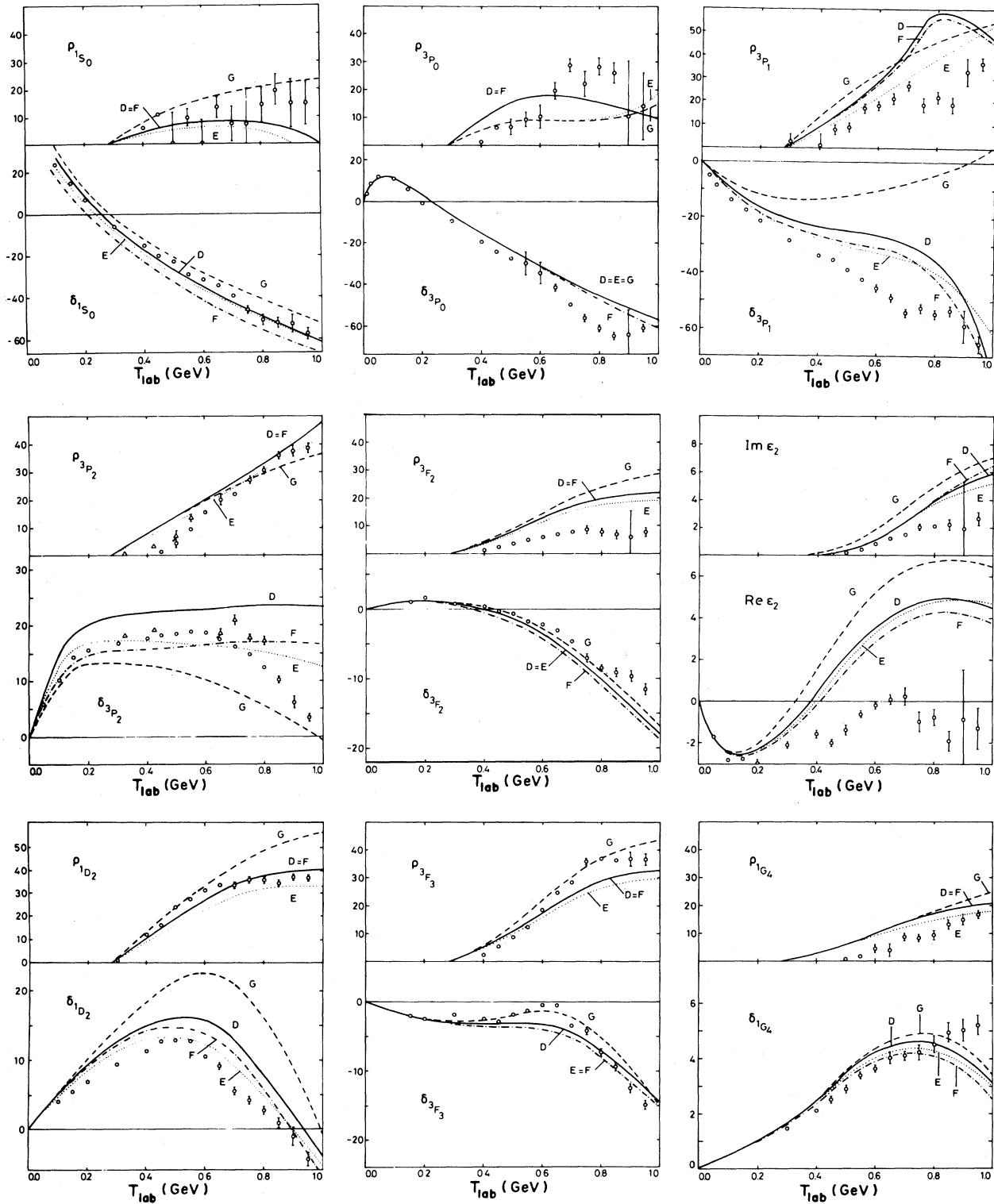


FIG. 3.  $T=1$  phase parameters  $\delta$  and  $\rho$  in degrees for  $f_{\pi\Delta}^2/4\pi=0.35$  and  $f_{\rho\Delta}^2/4\pi=8.0$ . ( $g_\epsilon^2/4\pi$ ,  $\Lambda_{N\Delta}^2/m^2$ ) is (6.7, 1.5) for curve D, (6.7, 1.0) for curve E, and (5.9, 1.5) for curve F. Curve G is obtained with (5.9, 1.0) and  $\rho N\Delta$  coupling set to zero. Experimental phase shift data are as in Fig. 2.

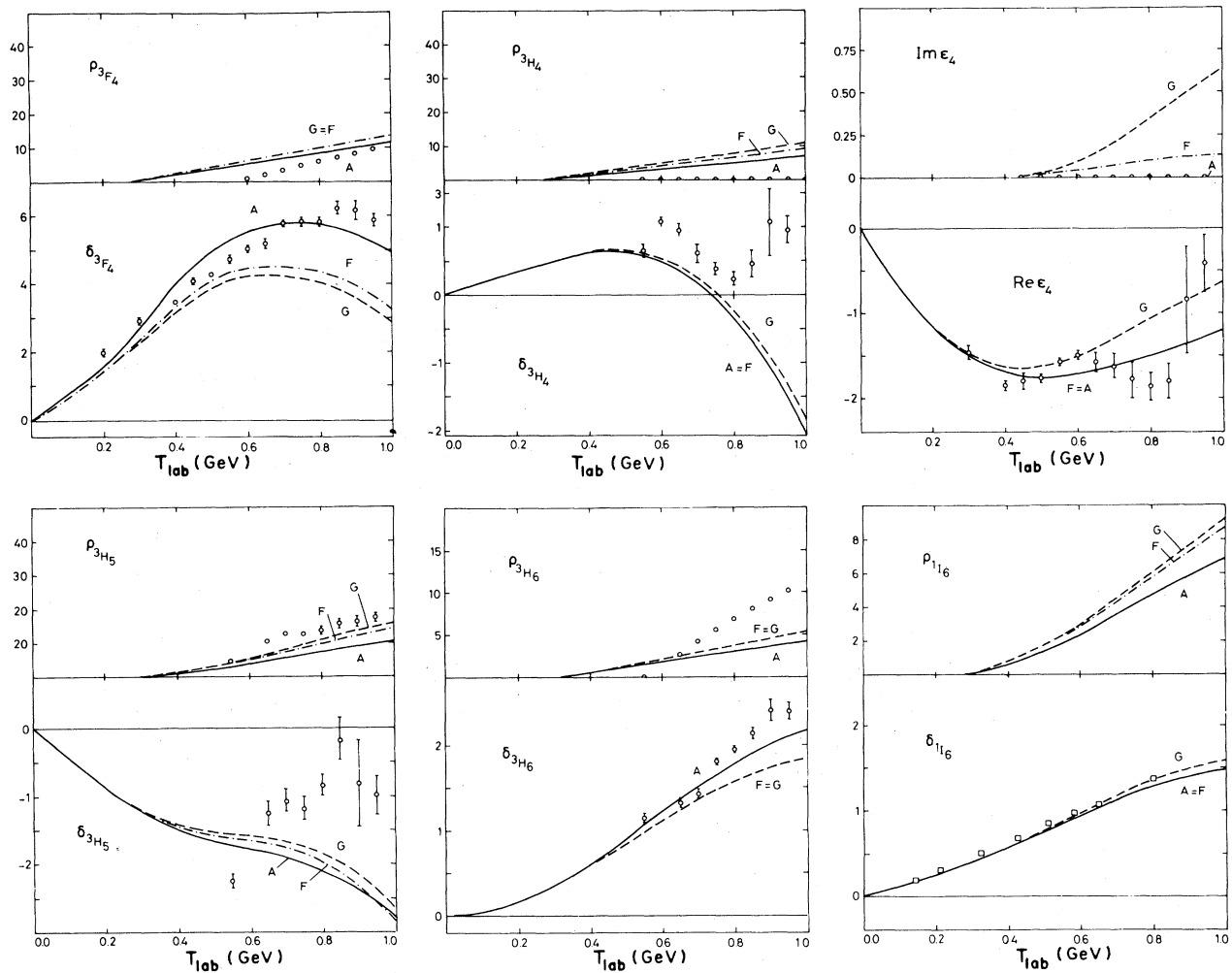


FIG. 4.  $T=1$  NN phase parameters  $\delta$  and  $\rho$  in degrees for higher partial waves. Alphabetical labeling of the curves is as in Figs. 2 and 3. Experimental phase shift data are taken from Ref. 3 (open circles) and Ref. 26 (open squares).

the experimental phase shifts we have used the data of Ref. 24. The latter show a tangible difference with Ref. 3 for the  $J=2$  coupled triplet and have therefore been included for these waves (triangles). Again agreement with experiment is improved if the  $\rho$  exchange is included in the transition interaction, although  $\epsilon_2$  still rises too fast. With the larger  $\pi N\Delta$  coupling constant the resonancelike behavior for  ${}^1D_2$  and  ${}^3F_3$  has become more prominent. In accordance, the inelasticities for these waves have increased.

In general, our model admits better fits to phase shift analyses than three-body calculations. The main reason is the inclusion of  $\rho N\Delta$  coupling, which is particularly important in getting the  $P$ -waves right. A second reason is the more elaborate treatment of the two-nucleon interaction. Both aspects have been implemented by other authors: Apart from  $P$  waves our results on inelasticities for  $f_{\pi\Delta}^2/4\pi=0.35$  are in accordance with those from the coupled channel calculations of Green and Sainio.<sup>28</sup> Agreement with Gruben and VerWest<sup>29</sup> is poor and our inelasticities are consistently larger for  $J \geq 3$ . Explicit calculation

shows that this cannot be caused by their different parametrization of the  $\Delta$  width, nor by their Born approximation for the  $NN \rightarrow NN\pi$  amplitude. However, a large part of the difference can be explained from the different  $\pi N\Delta$  coupling constants used in the various calculations, at least in the higher energy region. This is shown in Fig. 5 for the case of  ${}^1G_4$ .

It is interesting to note the sudden onset of inelasticity at pion production threshold. Figure 6 shows  ${}^1S_0$  as an example. For this particular channel one would expect a slower onset from the fact that it couples to an  $l=2$   $N\Delta$  state. The agreement with calculations by Green and Sainio<sup>28</sup> suggests that this is a common feature of models which incorporate pion production by using a one particle model for the isobar with energy dependent width.

## VII. CONCLUDING REMARKS

Using a relativistic one boson exchange model with  $\Delta$  degrees of freedom, the effect of  $\rho$  exchange in the transi-

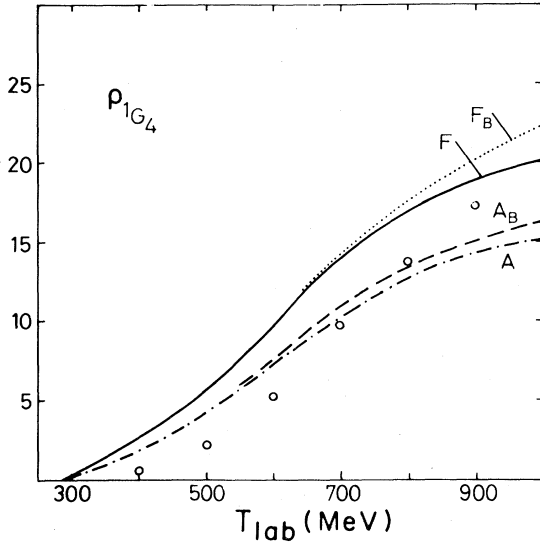


FIG. 5. Inelastic phase parameter  $\rho$  in degrees for  ${}^1G_4$ . Curves A and F are identical to those in Figs. 2 and 3.  $A_B$  and  $F_B$  show the corresponding contributions from the  $N\Delta$  box only. Open circles give results from Ref. 29.

tion interaction on the phase parameters of NN scattering in the  $I=1$  channels has been studied. Owing to the state dependence of the  $\rho$  exchange force a marked improvement is found for the  $P$  waves. Although the effects of  $\rho N\Delta$  coupling in general is to weaken the  $\pi N\Delta$  interaction at shorter distances, notable exceptions are found for the  ${}^3P_2$  and  ${}^3F_4$  channels.

Considering the  ${}^1D_2$  and  ${}^3F_3$  waves in the presence of the coupling to the  $N\Delta$  channels the resonancelike structures around  $T_{\text{lab}}=600$  MeV are reproduced. The maximum in the phase shift of the  ${}^3F_3$  wave is, however, not as pronounced as compared to the experiment if the  $\rho N\Delta$  coupling is included (see Fig. 3). This indicates that a

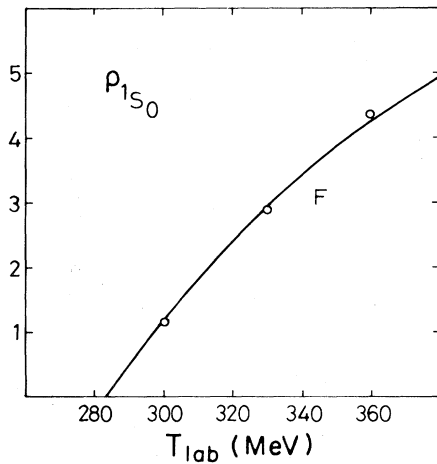


FIG. 6. Onset of inelasticity at pion production thresholds for  ${}^1S_0$ . Curve F is identical to those in Figs. 3 and 5. Open circles give results from Ref. 28.

stronger coupling to the inelastic channels is needed than we have used here, or possibly that other inelastic effects should be taken into account in this channel.

The question whether the resonancelike structures can be interpreted as dynamical singularities in the second Riemann sheet of the  $s$  variable or as threshold behavior effects has not been studied by us in this model. However, since the latter has the same physical ingredients as the model in Ref. 30, we expect that a similar conclusion also holds in our case, i.e., the structures are a combined effect of threshold behavior (pseudoresonance effect) and the presence of dynamical singularities originating from the one pion pole in the driving force. In this context it should be remarked that the  $N\Delta$  box diagram will inherently lead to pseudoresonance behavior irrespective of the coupling type or particular channel involved. For higher partial waves, especially those like  ${}^1G_4$ , the Argand plot indeed shows counterclockwise looping. However, for low partial waves like  ${}^3P_1$ , the effect of the  $N\Delta$  box may not be seen due to the contributions from the strong NN interaction.

#### ACKNOWLEDGMENTS

We would like to thank Dr. W. M. Kloet for helpful discussions. This work received partial financial support from the Nederlandse Organisatie voor Zuiver Wetenschappelijk Onderzoek, administered through the foundation Fundamenteel Onderzoek der Materie (FOM).

#### APPENDIX A

The wave function of the spin  $\frac{3}{2}$   $\Delta$  isobar can be found by assuming it to be constructed from a spin 1 and a spin  $\frac{1}{2}$  particle. Choosing the  $z$  axis parallel to the three momentum  $k$ , the spin 1 states are

$$\begin{aligned} \epsilon_1^\mu &= - \left[ 0, \frac{1}{\sqrt{2}}, \frac{i}{\sqrt{2}}, 0 \right], & \epsilon_2^\mu &= \left[ 0, \frac{1}{\sqrt{2}}, \frac{-i}{\sqrt{2}}, 0 \right], \\ \epsilon_3^\mu &= \left[ \frac{k}{m}, 0, 0, \frac{E_k}{m} \right], \end{aligned} \quad (\text{A1})$$

with  $k_\mu \epsilon_i^\mu = 0$  and  $\epsilon_i^\mu (\epsilon_j^\mu)^* = -\delta_{ij}$ . The spin  $\frac{1}{2}$  components are Dirac spinors with a normalization chosen according to Kubis,<sup>31</sup>

$$\begin{aligned} U_+ &= \begin{pmatrix} 1 \\ 0 \\ \frac{k}{E_k + m} \\ 0 \end{pmatrix} \left[ \frac{E_k + m}{2E_k} \right]^{1/2}, \\ U_- &= \begin{pmatrix} 0 \\ 1 \\ 0 \\ -k \\ \frac{E_k + m}{E_k + m} \end{pmatrix} \left[ \frac{E_k + m}{2E_k} \right]^{1/2}, \end{aligned} \quad (\text{A2})$$

satisfying  $\bar{U}U = (m/E_k)\delta_{\sigma\sigma'}$  and  $U^\dagger U = \delta_{\sigma\sigma'}$ .

Combining these basic wave functions with the appropriate Clebsch-Gordan coefficients we immediately find the expressions for the Rarita-Schwinger vector spi-

TABLE III. Isospin factors for transition amplitudes.

	$T=0$	$T=1$
NN $\leftrightarrow$ NN	-3	1
NN $\leftrightarrow$ N $\Delta$	0	$-\sqrt{8/3}$
N $\Delta$ $\leftrightarrow$ N $\Delta$	0	$-\frac{1}{3}$

nors  $\Delta^\mu$ , with spin components from  $-\frac{3}{2}$  to  $+\frac{3}{2}$ :

$$\Delta_{3/2}^\mu = \epsilon_1^\mu U_+, \quad \Delta_{-1/2}^\mu = \frac{1}{\sqrt{3}} \epsilon_2^\mu U_+ + \left(\frac{2}{3}\right)^{1/2} \epsilon_3^\mu U_-, \quad (\text{A3})$$

$$\Delta_{1/2}^\mu = \frac{1}{\sqrt{3}} \epsilon_1^\mu U_- + \left(\frac{2}{3}\right)^{1/2} \epsilon_3^\mu U_+, \quad \Delta_{-3/2}^\mu = \epsilon_2^\mu U_- .$$

The mass  $m$  appearing in Eq. (A2) must now of course be taken as the real part of the  $\Delta$  mass.

In this form the vector index has been retained, and the spinor index suppressed. The behavior under Lorentz transformations is found by the observation that the wave functions transform as a four-vector on the vector indices, and as an ordinary Dirac spinor on the (suppressed) spinor index. The vector spinors are normalized according to

$$(\bar{\Delta}_\sigma)_\mu (\Delta_{\sigma'})^\mu = -\delta_{\sigma\sigma'} \frac{m}{E_k}, \quad (\text{A4})$$

$$(\Delta_\sigma^\dagger)_\mu (\Delta_{\sigma'})^\mu = -\delta_{\sigma\sigma'} .$$

The two particle wave functions  $\psi(\rho_1 \lambda_1 \lambda_2)$  are defined in the c.m. frame according to the helicity formalism of Jacob and Wick<sup>19</sup> (take  $\vec{p}$  along the  $z$  axis),

$$\psi(\rho \lambda_1 \lambda_2) = U(1, p_1 \lambda_1) V(2, p_1 \lambda_2) \quad (\text{A5})$$

with

$$V(2, p_1 \lambda_2) \equiv (-)^{s_2 - \lambda_2} e^{-i\pi J_y} U(2, p_1 \lambda_2) \quad (\text{A6})$$

and where  $s_2$  is the spin of particle 2. [The phase factor for  $V$  has been chosen in such a way that  $V(2, 0, \lambda_2)$  reduces to  $U(2, 0, -\lambda_2)$ .] States with arbitrary direction of  $p$  are generated by rotations of  $\psi(p, \lambda_1 \lambda_2)$ :

$$|p, \theta, \varphi \lambda_1 \lambda_2\rangle \equiv e^{-i\varphi J_z} e^{-i\theta J_y} e^{i\varphi J_z} \psi(p, \lambda_1 \lambda_2), \quad (\text{A7})$$

where  $J_i = J_i^{(1)} + J_i^{(2)}$ . The explicit form of particle type 2 Dirac spinors is found from the definition (A6):

$$V_+ = \begin{pmatrix} 0 \\ 1 \\ 0 \\ k \\ E_k + m \end{pmatrix} \left[ \frac{E_k + m}{2E_k} \right]^{1/2}, \quad (\text{A8})$$

$$V_- = \begin{pmatrix} 1 \\ 0 \\ -k \\ E_k + m \\ 0 \end{pmatrix} \left[ \frac{E_k + m}{2E_k} \right]^{1/2} .$$

Similarly the  $\Delta$  vector spinors of type 2 are found to be

$$D_{3/2}^\mu = \epsilon_2^\mu V_+, \quad D_{1/2}^\mu = \frac{1}{\sqrt{3}} \epsilon_2^\mu V_- - \left(\frac{2}{3}\right)^{1/2} \epsilon_4^\mu V_+, \quad (\text{A9})$$

$$D_{-1/2}^\mu = \frac{1}{\sqrt{3}} \epsilon_1^\mu V_+ - \left(\frac{2}{3}\right)^{1/2} \epsilon_4^\mu V_-, \quad D_{-3/2}^\mu = \epsilon_1^\mu V_- ,$$

where

$$\epsilon_4^\mu = \left[ \frac{k}{m}, 0, 0, \frac{-E_k}{m} \right]$$

and  $\epsilon_i^\mu$ ,  $i=1,2,3$  are defined in Eq. (A1).

The normalization  $M$  of a general two particle state is

$$M = \langle \vec{p}'_1 \vec{p}'_2 \mu'_1 \mu'_2 | \vec{p}_1 \vec{p}_2 \mu_1 \mu_2 \rangle \\ = \delta_{\mu_1 \mu'_1} \delta_{\mu_2 \mu'_2} \delta^3(\vec{p}_1 - \vec{p}'_1) \delta^3(\vec{p}_2 - \vec{p}'_2) \cdot N_1 N_2 ; \quad (\text{A10})$$

here  $N_i$  denotes the spinor norm:

$$N_i = U^\dagger(p_i) U(p_i) = 1 \quad \text{for nucleons,} \\ = -1 \quad \text{for } \Delta \text{ isobars} \quad (\text{A11})$$

[the peculiar sign is due to the vector component normalization (A4)]. In the c.m. system  $\vec{p}_1 = -\vec{p}_2 = (p_1, \theta, \varphi) = (p_1, \Omega)$ , the normalization of NN states is:

$$M = \langle p' \Omega' \mu'_1 \mu'_2 | p \Omega \mu_1 \mu_2 \rangle \\ = \delta_{\mu_1 \mu'_1} \delta_{\mu_2 \mu'_2} \frac{2}{p E_p} \delta^2(\Omega - \Omega') \delta^4(P - P'), \quad (\text{A12})$$

where  $P \equiv p_1 + p_2$ .

## APPENDIX B: ISOSPIN FACTORS

The isospin structure of N $\Delta$  coupling appears as an overall factor for the transition amplitude. Using the Wigner-Eckart theorem the factor for given total isospin  $T$  can be written as a Wigner  $6J$  symbol:

$$\text{factor} = [(2I'_1 + 1)(2I'_2 + 1)]^{1/2} (-)^{T+I_1+I'_2} \begin{Bmatrix} I_1 & 1 & I'_1 \\ I'_2 & T & I_2 \end{Bmatrix} F(I'_1, I_1) F(I'_2, I_2) . \quad (\text{B1})$$

Here  $I_1$  ( $I'_1$ ) and  $I_2$  ( $I'_2$ ) are the isospins of the incoming (outgoing) particles 1 and 2, respectively. Here  $F$  denotes the re-

duced matrix element from the Wigner-Eckart theorem. Customarily this element is taken as 1 for  $N\Delta$  vertices and  $\sqrt{3}$  for  $NN$  vertices (the latter factor leads to the Pauli spin matrices). The form given above is seen to be valid for  $NN \leftrightarrow NN$  and  $NN \leftrightarrow N\Delta$  transitions, where a number 1 particle couples to another number 1 particle. This is not the case for  $N\Delta \leftrightarrow N\Delta$  amplitudes where a number 1 particle is coupled onto a number 2 particle. For this case

$$\begin{aligned} \text{factor} &= \sum_{l=-1}^1 (-)^l \sum_{\lambda\lambda'} \begin{pmatrix} \frac{3}{2} & \frac{1}{2} & T \\ \lambda & m-\lambda & m \end{pmatrix} \begin{pmatrix} \frac{3}{2} & \frac{1}{2} & T \\ \lambda' & m-\lambda' & m \end{pmatrix} \begin{pmatrix} \frac{3}{2} & 1 & \frac{1}{2} \\ \lambda & l & m-\lambda' \end{pmatrix} \begin{pmatrix} \frac{1}{2} & 1 & \frac{3}{2} \\ m-\lambda & -l & \lambda' \end{pmatrix} \\ &= -\frac{1}{3} \delta_{T,1}. \end{aligned} \quad (\text{B2})$$

No reduced matrix elements appear now since we have  $N\Delta$  vertices only. The isospin factors from (B1) and (B2) are given in Table III ( $T=2$  is inaccessible for  $NN$  scattering).

### APPENDIX C: EVALUATION OF TRANSITION AMPLITUDES IN TERMS OF LEGENDRE FUNCTIONS

Consider an arbitrary spinor matrix element in Eq. (32),

$$R = {}_i \langle \theta 0 \mu'_1 \mu'_2 | V | 0 0 \mu_1 \mu_2 \rangle_j. \quad (\text{C1})$$

It contains kinematical singularities through the dependence on  $\sin\theta/2$  and  $\cos\theta/2$ , which can be explicitly factored out. From inversion of Eq. (32),  $R$  can be written as

$$R = \sum_{j=0}^{\infty} \frac{2J+1}{4\pi} A_{ij}(\mu'_1 \mu'_2 | \mu_1 \mu_2) d_{\mu\mu'}^J(\theta) \quad (\text{C2})$$

with  $\mu = \mu_1 - \mu_2$  and  $\mu' = \mu'_1 - \mu'_2$ . In view of the symmetry relation

$$\begin{aligned} d_{\mu\mu'}^J(\theta) &= (-)^{\mu' - \mu} d_{-\mu', -\mu}^J(\theta) \\ &= (-)^{\mu' - \mu} d_{\mu\mu'}^J(\theta) \end{aligned} \quad (\text{C3})$$

we may only consider  $\mu \geq \mu'$ ,  $\mu \geq 0$ . Then (cf. Ref. 32, p. 58)

$$\begin{aligned} d_{00}^J(\theta) &= P_J, \quad \sin\theta d_{10}^J(\theta) = \frac{\sqrt{J(J+1)}}{2J+1} (P_{J+1} - P_{J-1}), \\ (1 \pm \cos\theta) d_{1,\pm 1}^J(\theta) &= \frac{J}{2J+1} P_{J+1} \pm P_J + \frac{J+1}{2J+1} P_{J-1}, \\ \sin^2\theta d_{20}^J(\theta) &= \left[ \frac{(J+2)(J+1)}{J(J-1)} \right]^{1/2} \left[ \frac{J(J-1)}{(2J+1)(2J+3)} P_{J+2} - \frac{2J(J-1)}{(2J-1)(2J+3)} P_J + \frac{J(J-1)}{(2J+1)(2J-1)} P_{J-2} \right], \\ \sin\theta(1 \pm \cos\theta) d_{2,\pm 1}^J(\theta) &= \left[ \frac{J+2}{J-1} \right]^{1/2} \left[ -\frac{(J-1)(J+1)}{(2J-1)(2J+1)} P_{J-2} \mp \frac{J-1}{2J+1} P_{J-1} + \frac{3(J-1)}{(2J-1)(2J+3)} P_J \right. \\ &\quad \left. \pm \frac{J-1}{2J+1} P_{J+1} + \frac{J(J-1)}{(2J+1)(2J+3)} P_{J+2} \right], \\ (1 \pm \cos\theta)^2 d_{2,\pm 2}^J(\theta) &= \frac{J(J-1)}{(2J+1)(2J+3)} P_{J+2} \pm \frac{2J-2}{2J+1} P_{J+1} + 6 \frac{(J+2)(J-1)}{(2J-1)(2J+3)} P_J \\ &\quad \pm \frac{2J+4}{2J+1} P_{J-1} + \frac{(J+1)(J+2)}{(2J-1)(2J+1)} P_{J-2}. \end{aligned}$$

These relations are used to express the partial wave amplitudes Eq. (32) in terms of  $Q_l$  functions.

$$d_{\mu\mu'}^J(\theta) \sim \cos^{\mu^+}(\theta/2) \sin^{\mu^-}(\theta/2) P_{J-\mu}^{\mu^-, \mu^+}(\cos\theta), \quad (\text{C4})$$

where  $\mu^{\pm} = \mu \pm \mu'$  and  $P_{J-\mu}^{\mu^-, \mu^+}$  are the Jacobi polynomials which can be expressed in terms of Legendre polynomials. Hence, from (C2) and (C4) it follows that the angular structure of  $R$  is given by

$$R = \cos^{\mu^+}(\theta/2) \sin^{\mu^-}(\theta/2) f(\cos\theta). \quad (\text{C5})$$

For the spinor couplings in Sec. IV it is found by explicit evaluation that  $f$  has the form

$$f(\cos\theta) = (\kappa^2 - m_B^2)^{-1} G(\cos\theta), \quad (\text{C6})$$

where  $\kappa = k$  or  $\tilde{k}$  and  $G$  is a polynomial of at most third degree.

For the coupled  $NN-N\Delta$  problem the number of independent  $d_{\mu\mu'}^J$  functions is restricted by the symmetry relations (C4) and by the observation that

$$|\mu| = |\mu - \mu'| \leq 2.$$

In view of Eq. (C5) we see that Eq. (32) contains the product of a  $d$  function with the prefactor of  $f$  in Eq. (C5). This product can be expressed in terms of Legendre polynomials. In our case we have

- <sup>1</sup>A. Yokosawa, Phys. Rep. 64C, 47 (1980).  
<sup>2</sup>N. Hoshizati, Prog. Theor. Phys. 60, 1796 (1978).  
<sup>3</sup>R. A. Arndt *et al.*, Virginia Report No. VPISA-2 (82), 1982.  
<sup>4</sup>W. M. Kloet and R. R. Silbar, Nucl. Phys. A338, 281 (1980);  
A338, 317 (1980); Phys. Rev. Lett. 45, 970 (1980).  
<sup>5</sup>M. Araki, Y. Koike, and T. Ueda, Nucl. Phys. A389, 605  
(1982); M. Araki and T. Ueda, *ibid.* A379, 449 (1982).  
<sup>6</sup>Y. Avishai and T. Mizutani, Phys. Rev. C 27, 312 (1983); T.  
Mizutani *et al.*, Phys. Lett. 107B, 177 (1981).  
<sup>7</sup>B. Blankleider and I. R. Afnan, Phys. Rev. C 24, 1752 (1981).  
<sup>8</sup>K. Erkelenz, Phys. Rep. 13C, 191 (1974).  
<sup>9</sup>K. Holinde, Phys. Rep. 68C, 122 (1981).  
<sup>10</sup>M. M. Nagels, T. A. Rijken, and J. J. de Swart, Phys. Rev. D  
20, 1633 (1979).  
<sup>11</sup>J. Fleischer and J. A. Tjon, Phys. Rev. D 21, 87 (1980).  
<sup>12</sup>M. J. Levine, J. Wright, and J. A. Tjon, Phys. Rev. 154, 962  
(1966); 157, 1416 (1967).  
<sup>13</sup>J. Fleischer and J. A. Tjon, Nucl. Phys. B84, 375 (1975).  
<sup>14</sup>J. A. Tjon and E. van Faassen, Phys. Lett. 120B, 39 (1983).  
<sup>15</sup>B. J. Verwest, Phys. Rev. C 25, 482 (1982).  
<sup>16</sup>A. M. Green, J. A. Niskanen, and M. E. Sainio, J. Phys. G 4,  
1055 (1978).  
<sup>17</sup>M. J. Zuilhof and J. A. Tjon, Phys. Rev. C 24, 736 (1981).  
<sup>18</sup>A. M. Green and M. E. Sainio, J. Phys. G 8, 1337 (1982).  
<sup>19</sup>M. Jacob and G. C. Wick, Ann. Phys. (N.Y.) 7, 404 (1959).  
<sup>20</sup>H. Strubbe, Comput. Phys. Commun. 8, 1 (1974); 18, 1 (1979).  
<sup>21</sup>B. J. Edwards and A. N. Kamal, Can. J. Phys. 57, 659 (1979).  
<sup>22</sup>R. Bryan, Phys. Rev. C 24, 2659 (1981).  
<sup>23</sup>R. A. Arndt and L. D. Roper, Phys. Rev. D 25, 2011 (1982).  
<sup>24</sup>R. A. Arndt and B. J. VerWest, Texas A&M Report No.  
DOE/ER/0523-29, 1981.  
<sup>25</sup>G. E. Brown and W. Weise, Phys. Rep. 22C, 279 (1975).  
<sup>26</sup>R. Dubois *et al.*, Nucl. Phys. A377, 554 (1982).  
<sup>27</sup>H. Sugawara and F. von Hippel, Phys. Rev. 172, 1764 (1968).  
<sup>28</sup>A. M. Green and M. E. Sainio, J. Phys. G 5, 503 (1979).  
<sup>29</sup>J. H. Gruben and B. J. VerWest, Texas A&M Report No.  
DOE/ER/05223-44, 1982.  
<sup>30</sup>W. M. Kloet, J. A. Tjon, and R. R. Silbar, Phys. Lett. 99B, 80  
(1981); W. M. Kloet and J. A. Tjon, Nucl. Phys. A392, 271  
(1983).  
<sup>31</sup>J. J. Kubis, Phys. Rev. D 6, 547 (1972).  
<sup>32</sup>A. R. Edmonds, *Angular Momentum in Quantum Mechanics*  
(Princeton University Press, Princeton, N.J., 1957).